BNL-43107
1
To be presented at the 16th Course of the International School of Materials Science and Technology on "Earlier and Recent Aspects of Superconductivity," Erice, Italy, July 4-16, 1989.
CONF-8907139-3

Magnetic and Electronic Correlations in $YBa_2Cu_3O_{6+x}$

BNL--43107
DE89 017604

J. M. Tranquada

Physics Department, Brookhaven National Laboratory
Upton, New York, USA 11973

Abstract. $YBa_2Cu_3O_{6+x}$ is an antiferromagnetic insulator in its tetragonal phase at small x, and it becomes a superconducting metal in the large x orthorhombic phase. The transition between the two phases is controlled by the orientational ordering of CuO_x chain segments and dielectric screening by the BaO layers. In the orthorhombic phase, holes from the chains are transferred to the CuO_2 planes, and the superconducting transition temperature scales with the density of O $2p$ holes. The antiferromagnetic ordering in the tetragonal phase is dominated by localized Cu moments in the CuO_2 planes. The two-dimensional (2D) coupling between those spins is unusually strong. The interaction between nearest-neighbor planes is sufficiently strong that spins in bilayers remain highly correlated well above the Néel temperature. Long-range order is destroyed when a significant density of O $2p$ holes is present in the planes; however, there is evidence that Cu moments survive and interact in the metallic phase.

1. Introduction

Before theorists can come to a consensus on the electron-pairing mechanism responsible for superconductivity in the layered copper-oxide compounds (or even agree on the Hamiltonian that contains the necessary basic physics of the problem), it is necessary to have a clear picture of the electronic and magnetic structure of these materials in the normal state. It is now generally agreed that the crucial structural element for the unusual superconductivity is the CuO_2 plane: a square lattice of copper atoms with an oxygen bridging each pair of nearest-neighbor coppers. The first superconducting cuprate discovered [1], $La_{2-x}Ba_xCuO_4$,

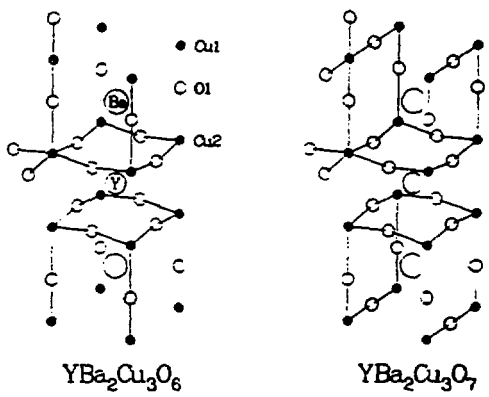

Fig. 1. Crystal structures of $YBa_2Cu_3O_6$, in which the Cu(1) sites are 2-fold coordinated, and $YBa_2Cu_3O_7$, in which the 4-fold coordinated Cu(1) sites form chains along the *b* axis.

contains only CuO_2 planes between layers of La(Ba)O. In the 90-K superconductor $YBa_2Cu_3CuO_7$ [2], however, each unit cell contains two CuO_2 planes plus a Cu layer in which oxygen bridges the Cu along just one direction, creating parallel CuO chains (see Fig. 1) [3]. The presence of the CuO chains causes the *b* lattice parameter (along the chain direction) to be longer than *a*, so that the structure is orthorhombic. When all of the oxygen is removed from the chains, as in $YBa_2Cu_3O_6$, the structure is tetragonal [4], and the material is an antiferromagnetic insulator [5, 6]. In the superconducting compound, the orthorhombic strain causes twinning: the chain direction can change by 90° at (110) boundaries between neighboring domains.

The presence of the chains and twin boundaries initially led to considerable confusion concerning the feature(s) responsible for the high superconducting transition temperature (T_c) in $YBa_2Cu_3O_7$. From a selective analysis of experimental results, it is now clear that it is the density of holes of predominantly O 2*p* character within the CuO_2 planes that determines T_c. The density of holes is controlled by the average occupancy x of the oxygen sites in the the CuO chain layer, and also the ordering of the oxygens on those sites. The distribution of holes between the chains and planes is stabilized electrostatically by displacements within the BaO layers. Furthermore, there is substantial evidence that the Cu atoms in the planes remain essentially 2+ (one 3*d* hole per Cu) in the presence of the O 2*p* holes, and that spin-spin interactions between neighboring Cu moments are significant in the metallic phase.

The experimentally determined phase diagram for $YBa_2Cu_3O_{6+x}$ is shown in Fig. 2. In the tetragonal phase the compound is an antiferromagnetic insulator, whereas it is a metallic superconductor when the lattice becomes orthorhombic. To understand the phase diagram it is

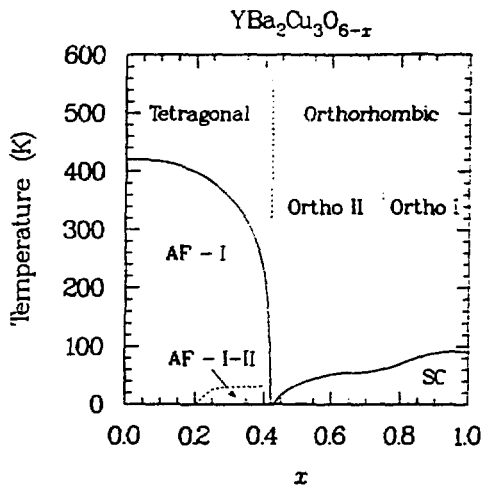

Fig. 2. Phase diagram of $YBa_2Cu_3O_{6+x}$. The positions of the phase boundaries with respect to x depend on sample preparation and treatment.

necessary to consider the connections between the crystalline, electronic, and magnetic structures. Some important features of the oxygen dependence of the crystal structure will be reviewed first, followed by a short description of variations in the electronic structure with x. Magnetic order and correlations will then be discussed, and the paper concludes with a summary.

2. Oxygen Dependence of the Crystal Structure

The filling and ordering of the Cu(1)-O_x chains control the filling of valence band states, and hence they control the electronic and magnetic properties of $YBa_2Cu_3O_{6+x}$. Copper finds it energetically favorable to be either linearly 2-fold or planar 4-fold coordinated by oxygen. A 4-fold coordinated Cu can tolerate one or two more distant oxygen neighbors, such as the apical O(1) near the Cu(2) in the CuO_2 planes (see Fig. 1), but 3-fold coordination is uncommon. Accepting these observations as rules, it is clear that for arbitrary x the oxygen in the Cu(1) planes will cluster into chains so as to maximize the number of 2- and 4-fold coordinated Cu(1) sites. If the orientational order to the chains is coherent from layer to layer, then the crystal will be orthorhombic; however, at small x, where the chain segments become shorter and more separated, the orientation may vary between layers or within a layer, and the average symmetry becomes tetragonal [7].

Because the full or empty chains may be charged, like-chains will tend to repel each other. As a result, a set of full and empty chains will

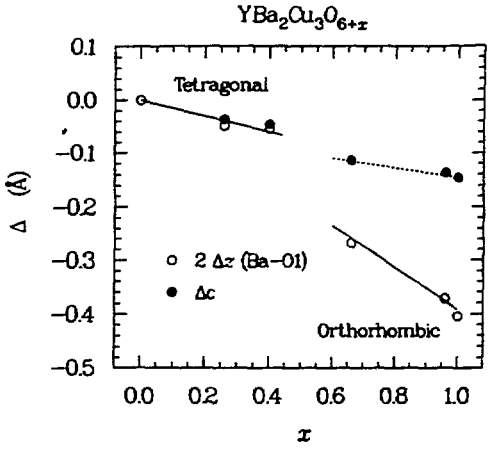

Fig. 3. Change in twice the Ba-O(1) intralayer spacing determined by neutron diffraction [3, 4] compared to the the change in the c lattice parameter as a function of x. Note that there are two BaO layers per unit cell.

tend to order themselves into a regular pattern. The dominant type of ordering observed by electron [8] and x-ray [9] diffraction for intermediate x consists of alternating full and empty chains, with a resultant doubling of the unit cell along the a axis. Theoretical model calculations [10] which reproduce this ordering indicate that there are two distinct orthorhombic phases: Ortho I, consisting of full chains plus defects, and Ortho II, corresponding to the cell-doubled phase. The equilibrium width in x of the Ortho II phase depends on sample treatment (annealing temperature and oxygen partial pressure) [11, 12].

As will be discussed in the next section, when oxygen atoms are added to an empty chain, they can obtain only half of the charge they require from their Cu(1) neighbors. Thus, either holes must be created in the chains, or electrons must be transferred from the planes to the chains, creating holes in the planes. Transferring electrons from the planes to the chains would change the electric field across the Ba-O(1) layer. The Ba and O(1) atoms are displaced from each other along the c-axis by an amount Δz(Ba-O1), and this separation contracts strongly with increasing x in the orthorhombic phase as shown in Fig. 3 [3, 4], consistent with plane-to-chain charge transfer [13]. Thus, the Ba-O(1) layer acts as a dielectric to screen the change in electric field due to the charge transfer. In the tetragonal phase the Ba-O(1) separation changes very little with x, suggesting that there is very little charge transfer. Thus, the density of holes in the planes should change in nearly a step-like way on going from the tetragonal to the orthorhombic phase.

3. Electronic Structure

It is now fairly well established that both the Cu(1) and Cu(2) atoms have a 2+ valence ($3d^9$ configuration) in the fully oxygenated $x = 1$ compound [14]. That the holes have a dominantly O $2p$ character is confirmed by x-ray absorption [15] and electron-energy-loss [16] measurements at the O K edge. The orientation dependence of O K edge measurements on single crystals indicate that the holes are shared between the chain and plane oxygens [17]. Evidence for O $2p$ holes in the planes and chains has also been obtained from nuclear magnetic resonance (NMR) studies probing ^{63}Cu [18], ^{17}O [19], and ^{89}Y [20] nuclei. Superconductivity occurs only when a significant density of holes is present in the planes. The hole density, and hence T_c, vary with x, and the details of that variation are controlled by the ordering of the oxygens in the Cu(1) layer.

If the oxygen atoms in the Cu(1) layer tend to cluster in chains, then there should be empty chain segments containing 2-fold coordinated Cu(1) for all $x < 1$. One expects these Cu(1) atoms to have a 1+ valence (i.e. a full $3d$ shell). A practical way to detect Cu(1)$^{1+}$ is through x-ray absorption measurements at the Cu K edge. As shown in Fig. 4, the $1s \rightarrow 4p_\pi$ transition for a Cu^{1+} ion, as in Cu_2O, is at a much lower energy than it is for Cu^{2+}, as in CuO. This low energy feature can be used as a fingerprint to indicate the presence of Cu^{1+}[21]. The lower part of Fig. 4 shows measurements on an oxygenated ($x = 1$) and an oxygen deficient ($x = 0.23$) sample, each of which had been uniaxially oriented in a magnetic field [22, 23]. Measurements with the x-ray polarization $\hat{\epsilon}$ parallel to and perpendicular to the c-axis of each sample reveal that the distinctive low energy Cu^{1+} feature is present only for the oxygen deficient sample with the polarization perpendicular to the c-axis. Since the Cu^{1+} $4p_\pi$ final state must be oriented perpendicular to the ligand axis [24], it is clear that the observed Cu^{1+} feature is due to 2-fold coordinated Cu(1) sites. The presence of Cu^{1+} in oxygen-deficient $YBa_2Cu_3O_{6+x}$ has also been detected and characterized by optical spectroscopy [25] and by nuclear quadrupole resonance (NQR) [26] and nuclear magnetic resonance (NMR) [27] spectroscopy.

A measure of the amount of Cu^{1+} present is given by the area under the low energy peak obtained after subtracting off the $x = 1$ spectrum. It can be put on an absolute scale by normalizing to the Cu_2O spectrum. Such an analysis has been performed on a series of unoriented samples having a range of x values [23], and the results are shown in Fig. 5. If

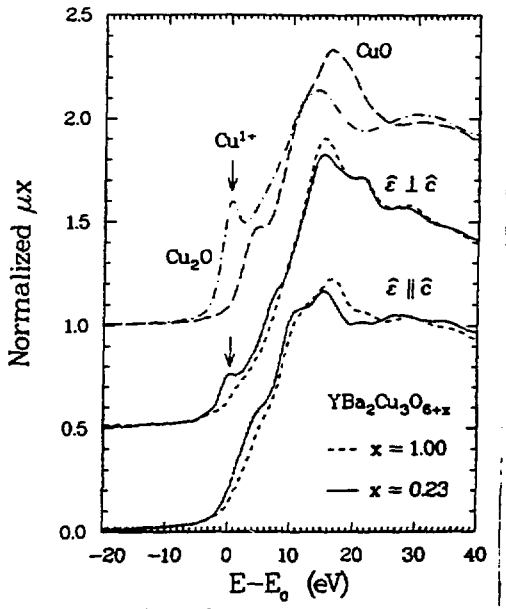

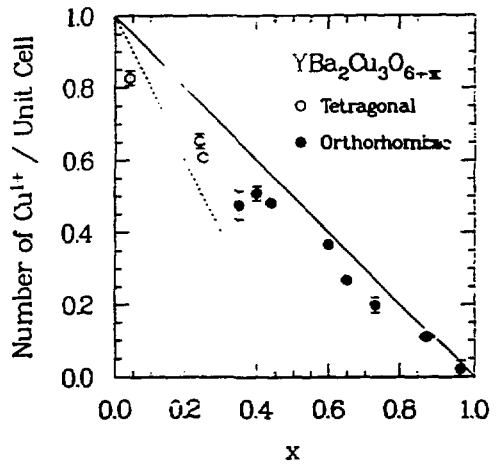

Fig. 4. (Left) X-ray absorption near edge structure measured at the Cu K edge, with $E_0 = 8980$ eV. At the top are data for unoriented powders of Cu_2O and CuO. Below are spectra, for uniaxially aligned samples of $YBa_2Cu_3O_{6+x}$ with $x = 0.23$ and 1.00, measured with the x-ray polarization vector $\hat{\varepsilon}$ perpendicular to and parallel to the c-axis direction $\hat{c}$. From Ref. [23].

Fig. 5. (Right) Number of Cu^{1+} ions per unit cell measured in $YBa_2Cu_3O_{6+x}$ plotted as a function of x. The solid line represents $n_{Cu^{1+}} = 1 - x$, while the dashed line indicates $n_{Cu^{1+}} = 1 - 2x$. From Ref. [23].

all of the Cu(1) atoms are in 2- or 4-fold sites, then the number of 2-fold sites is equal to $1 - x$, corresponding to the solid line in Fig. 5. The data are consistent with essentially all of the Cu(1) sites being in full or empty chains, with the atoms in empty chains having a valence of 1+.

It seems likely that the oxygen atoms cluster into chain segments in the tetragonal phase; however, it is interesting to consider another limit in which evergy oxygen is isolated and sits between two 3-fold coordinated Cu(1) atoms. If one assumes that the 3-fold sites have a 2+ valence, then the density of Cu^{1+} would be $1 - 2x$, corresponding to the dashed line in Fig. 5. Taking into account a possible systematic error in the normalization, the data appear more consistent with chain segments in the tetragonal phase.

From simple valence counting, the result that the density of $Cu(1)^{1+}$ atoms is equal to $1-x$ implies that the density of holes n_h is equal to x. For the quenched samples used in the Cu K edge study, it was observed that $T_c \sim x$ [23]. It follows that $T_c \sim n_h$. A similar result was obtained in a muon spin relaxation study [28]. By studying the relaxation rate for superconducting $YBa_2Cu_3O_{6+x}$ in an applied magnetic field, it was established that, at least for $x \lesssim 0.9$, $T_c \sim n_h/m^*$, where m^* is the effective mass of the holes. For annealed samples, a wide plateau develops at ~ 60 K in the T_c vs. x curve [11], corresponding to the Ortho II phase. It has been argued that the plateau structure is due to percolation effects resulting from the inhomogeneity of the chain ordering on the length scale of the superconducting coherence length (20–30 Å) [29].

4. Magnetic Structure and Excitations

In the fully reduced compound $YBa_2Cu_3O_6$ the Cu(2) sites in the planes have magnetic moments by virtue of their 2+ valence, while the 2-fold coordinated Cu(1) sites are nonmagnetic. The Cu moments within the CuO_2 planes order antiferromagnetically because of nearest-neighbor superexchange interactions, and the planes couple together antiferromagnetically along the c axis, as shown in Fig. 6(a) [6]. The magnetic Bragg peak intensity is proportional to the square of the staggered magnetization, which in turn is proportional to the average spin $\langle S \rangle$. Experimetally, a value of $M = g\mu_B\langle S \rangle \approx 0.65\mu_B$ was observed at low temperature [30, 31] where μ_B is the Bohr magneton. Assuming a typical value of $g \sim 2.2$ for a spin-$\frac{1}{2}$ Cu^{2+}ion, one obtains $\langle S \rangle \approx 0.30$. As will be discussed below, the magnetic interactions within the CuO_2 planes are much stronger than those between the planes, and it is commonly believed that the spin dynamics should be very similar to those of a 2D Heisenberg system. Because of the very small size of the spin, quantum corrections become important, and a large zero-point spin fluctuation is expected. Spin-wave analysis applied to the spin-$\frac{1}{2}$, 2D Heisenberg model yields $\langle S \rangle = 0.30$ [32], in very good agreement with the experimental result. Thus, the neutron diffraction results are consistent with localized magnetic moments of approximately 1 μ_B and large fluctuations in spin orientation even at low temperatures.

The temperature dependence of the magnetic ordering has been studied as a function of oxygen content x by muon spin rotation [33], neutron

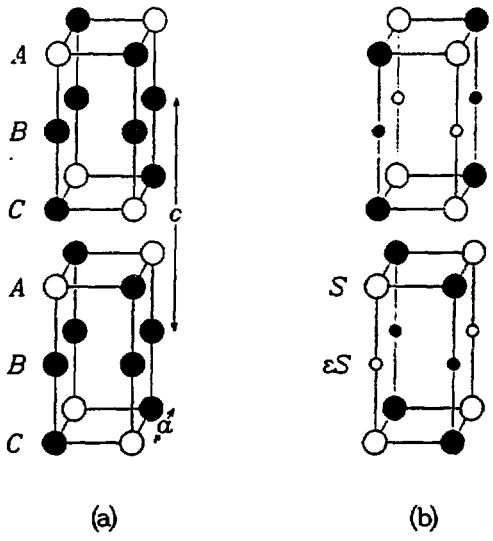

Fig. 6. (a) Magnetic spin structure for $YBa_2Cu_3O_{6+x}$ with x near zero. Only copper atoms are shown for clarity; cross-hatched circles represent nonmagnetic Cu^{1+} ions, while black and white circles indicate antiparallel spins at Cu^{2+} sites. Solid lines connect pairs of sites bridged by oxygen atoms. (b) Second type of spin structure expected for larger x. The average spin at a B-layer site is a fraction ϵ of the spin on a CuO_2 layer.

diffraction [30, 31], and Cu NQR [34], and the results are summarized by the magnetic phase boundaries shown in Fig. 2. With increasing x, oxygen enters the Cu(1) layer and creates some $Cu(1)^{2+}$. Clustering of oxygen into chains should also create some holes, but very few of these are transferred to the CuO_2 planes, as discussed in the previous two sections. This conclusion is confirmed by the observation that T_N stays fairly high over a large range of x, in contrast to $La_{2-x}Sr_xCuO_{4-y}$ in which a very small amount of doping destroys the long-range order [35]. In $YBa_2Cu_3O_{6+x}$ the magnetic order is not destroyed by mobile holes until the tetragonal-orthorhombic phase boundary is reached. The magnetic $Cu(1)^{2+}$ ions are frustrated in the Type II structure of Fig. 6(a). By Hund's rules, one expects the Cu(1) to couple ferromagnetically to its Cu(2) neighbors [36, 37], causing the Cu(2) spins in next-nearest-neighbor planes to be ferromagnetically aligned. When a sufficient number of moments are present on Cu(1) sites, one would expect the Type II structure of Fig. 6(b) to be favorable [38]. The average Cu(1) spin should be much smaller than the average Cu(2) spin.

Superlattice peaks corresponding to the Type II structure were observed to coexist with Type I peaks below 40 K in one single crystal with $x \sim 0.35$ studied by neutron diffraction [39]. As the temperature decreased below 40 K, the intensities of the Type I peaks decreased while the Type II peaks grew. A more common observation in single crystal diffraction studies is that, for $x \gtrsim 0.2$, the Type I magnetic Bragg peaks begin to decrease as the temperature is lowered below 30–50 K [see Fig. 7(a)], but instead of new superlattice peaks appearing, 2D diffuse

scattering is found [31, 40]. Furthermore, there is a low energy component to the inelastic scattering which is in excess of that expected for the temperature dependence of spin-waves from the CuO_2 layers, as shown in Fig. 7(b) and (c). The intensity of the low-energy scattering reaches a maximum in the temperature range where the magnetic Bragg intensity begins to decrease, suggesting that it is due to critical fluctuations of $Cu(1)^{2+}$ moments whose spin direction freezes at low temperature. Similarly, a recent magnetic susceptibility study [41] has revealed a Curie-like contribution that increases in magnitude with x up to the tetragonal-orthorhombic phase boundary, but which disappears below 20–30 K. Evidence for a low-temperature transition to a spin-glass-like phase comes from Cu NQR measurements. For $x \geq 0.2$, the spin-echo decay rate for the NQR for $Cu(1)^{1+}$ diverges at 20 K [42]. A single broad peak is observed at low temperature. If the low-temperature magnetic structure were of Type II, then all Cu(1) sites should see the same constant hyperfine field, and the $Cu(1)^{1+}$ peak should be split in two. In the only case where such a splitting was observed, the sample was found to contain a small amount of Fe impurity [43], which tends to substitute on the Cu(1) site. Substituting magnetic Co ions on Cu(1) sites also induces Type II order [44]. The Type II order observed in $Nd_{1+y}Ba_{1-y}Cu_3O_{6+x}$ [45] is probably caused by the presence of excess Nd^{3+} on Ba^{2+} sites.

The evidence indicates that the $Cu(1)^{2+}$ moments do order in some way at low temperature, but that they do not exhibit the coherent order of the Type II structure. If random Cu(1) layers couple to the planes with local Type II structure, then a mixture of Type I and Type II structures could form, as illustrated in Fig. 8. Isolated Type II layers would contribute diffuse rather than Bragg scattering, and their presence would reduce the number of CuO_2 planes contributing to the Type I superlattice peaks. Most $Cu(1)^{1+}$ sites would see no hyperfine field, consistent with the Cu NQR results.

A classical antiferromagnet would have perfect Néel order at zero temperature. At a finite temperature the spins will fluctuate around their zero temperature orientations, and these fluctuations can be analyzed in terms of harmonic spin waves. In a quantum mechanical antiferromagnet spin waves are present even at $T = 0$, and correspond to the zero-point fluctuations of the spins. In a nearest-neighbor Heisenberg model, the Hamiltonian for spin-spin interactions has the form

$$H = J \sum_{\langle i,j \rangle} \mathbf{S}_i \cdot \mathbf{S}_j,$$

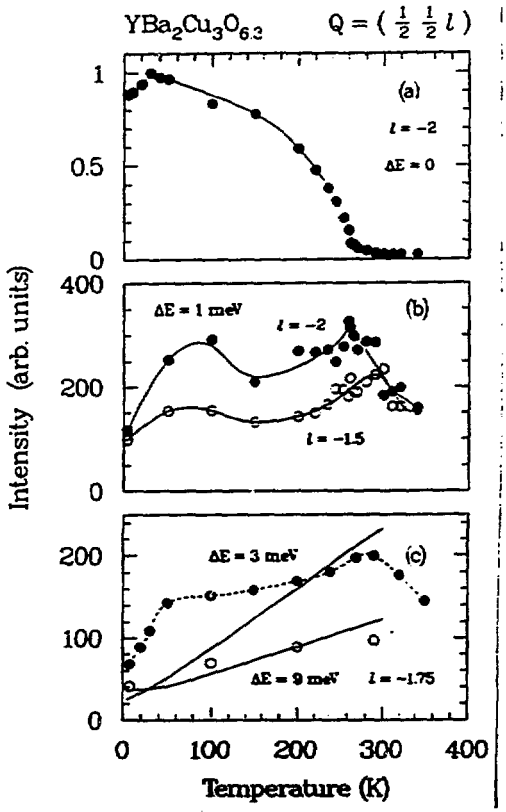

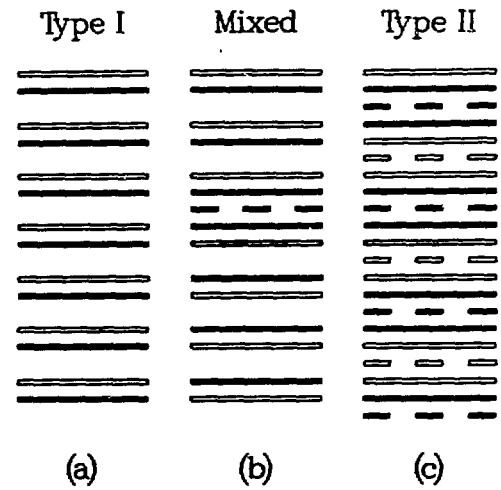

Fig. 7. (Left) Temperature dependence of elastic and inelastic magnetic scattering in $YBa_2Cu_3O_{6.3}$. (a) Elastic Bragg peak intensity at $(\frac{1}{2},\frac{1}{2},-2)$. (b) Inelastic intensity for $\Delta E = 1$ meV at $(\frac{1}{2},\frac{1}{2},-2)$ and $(\frac{1}{2},\frac{1}{2},-1.5)$. (c) Background corrected inelastic intensity at $(\frac{1}{2},\frac{1}{2},-1.75)$ for $\Delta E = 3$ and 9 meV. the solid lines represent the calculated temperature dependence normalized to the 9 meV point at 200 K, taking the spectrometer resolution function into account; the dashed line is a guide to the eye. From Ref. [40].

Fig. 8. (Right) Schematic diagrams of different magnetic structures, as discussed in the text. Each bar represents an antiferromagnetic CuO_2 plane in which the Cu spins have a simple Néel order. Black and white bars indicate layers with antiparallel spoins. Broken bars represent magnetically ordered Cu(1) layers. From Ref. [40].

where the sum is over nearest-neighbor pairs and J is called the exchange energy. Diagonalization of the Hamiltonian leads to a dispersion relation for the spin-wave energy $\hbar\omega$ as a function of wavevector q, measured

relative to a magnetic Bragg point. For small q the dispersion is linear, with a velocity $c = \omega/q$ proportional to the exchange energy J. Hence, by measuring the slope of the spin-wave dispersion with inelastic neutron scattering one can determine the strength of coupling between the spins.

Anderson [46] was the first to point out that the superexchange interaction between nearest-neighbor coppers within a CuO_2 plane should be unusually strong, and that the magnetism should be essentially two-dimensional in character. These speculations were initially confirmed by neutron scattering studies of La_2CuO_4 [47]. For a 2D system, the scattering cross section does not depend on the momentum transfer perpendicular to the plane, so that in reciprocal space Bragg points are replaced by Bragg rods. Figure 9 shows the (hhl) zone in reciprocal space for $YBa_2Cu_3O_{6+x}$, with the rod for antiferromagnetic scattering from a CuO_2 layer indicated by the hatched line. Below T_N, magnetic Bragg peaks are observed at the points indicated by the squares. Assuming that the spin dynamics are dominated by the exchange energy $J_{||}$ between nearest-neighbors within a CuO_2 plane, one expects to observe spin waves rising steeply in energy as q is scanned in the $[hh0]$ direction away from the 2D rod, as indicated by Scan A in Fig. 9. In an inelastic neutron scattering measurement, if one fixes the energy transfer $\Delta E = \hbar\omega$ and performs Scan A, spin wave peaks should be observed at $q_{||} = \pm\omega/c$, where $q_{||}$ is the component of q perpendicular to the rod. Such scans, with $\Delta E = 3$, 9, and 15 meV and measured on a single crystal with $x \sim 0.3$, are shown in Fig. 10. Because of the very large spin-wave velocity, the two spin-wave peaks cannot be resolved. By taking into account the spectrometer resolution function, one can fit the unresolved peaks as indicated by the solid lines, yielding the crude estimate $J_{||} = 80^{+60}_{-30}$ meV. Inelastic light-scattering measurements of spin-pair excitations indicate that $J_{||} \approx 120$ meV in a single crystal with $x \approx 0.0$ [48].

If the CuO_2 layers were truly uncoupled, then there would be no spin-wave dispersion along the $[00l]$ direction indicated by Scan B in Fig. 9. In reality, the Cu spins are coupled weakly along the c axis, and because there are two Cu(2) atoms per unit cell, the spin-wave modes are split into acoustic and optical branches, in analogy with phonon modes in a non-Bravais lattice. Two different c-axis couplings must be considered: $J_{\perp 1}$, between nearest-neighbor (nn) CuO_2 planes, and $J_{\perp 2}$, between next-nn layers through the Cu(1) sites. It turns out that the direct exchange interaction corresponding to $J_{\perp 1}$ is much stronger than $J_{\perp 2}$. As a result, $J_{\perp 1}$ determines the zone-center splitting of the acoustic and optical

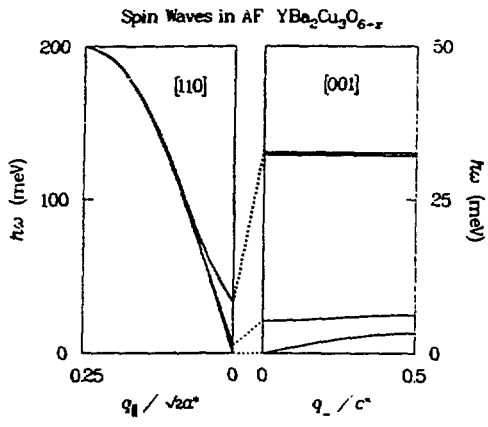

Fig. 11. Schematic diagram of spin-wave dispersion in $YBa_2Cu_3O_{6+x}$. Note that the energy scales for the two panels differ by a factor of four. The 2D nature of the magnetic interactions makes the dispersion very large along $q_\parallel$ but extremely weak along $q_\perp$. From Ref. [40]

and where $z = 0.28$ is the relative separation between nn Cu(2) sites along the c axis [40, 49]. Figure 12 shows scans along the $(\frac{1}{2}\frac{1}{2}l)$ direction at $\Delta E = 6$ meV for several different temperatures [40]. The solid line is a fit using spin-wave theory and taking the spectrometer resolution function into account. The phase and amplitude of the modulation make it clear that only acoustic modes contribute to the scattering. Quite remarkably, the structure factor modulation is still present well above T_N, indicating that CuO_2 bilayers remain strongly correlated in the absence of three-dimensional order. The optical modes are not observed up to at least 30 meV, providing the limit $J_{\perp 1} \gtrsim 2$ meV [40]. $J_{\perp 2}$ and the exchange anisotropy are much smaller, being on the order of $10^{-4} \times J_\parallel$.

What happens to the magnetic moments in the metallic orthorhombic phase of $YBa_2Cu_3O_{6+x}$? As discussed in the previous section, high-energy spectroscopies indicate that the Cu(2) atoms retain their 2+ valence for all x, suggesting that they should remain magnetic. Temperature-dependent magnetic susceptibility measured for varying oxygen content and corrected for a small Curie-like contribution is shown in Fig. 13 [30, 50]. At low temperatures the susceptibility has the shape expected for a 2D antiferromagnet [51], and it appears to evolve continuously as the boundary between the antiferromagnetic and the metallic phases is crossed. A much more drastic change would be expected if the magnetic moments and/or the correlations suddenly disappeared in the orthorhombic phase.

The results of neutron scattering searches for low energy magnetic scattering have been mixed so far. Mezei *et al.* [52] observed a magnetic cross section at very low energies (≤ 1.5 meV) and low temperature

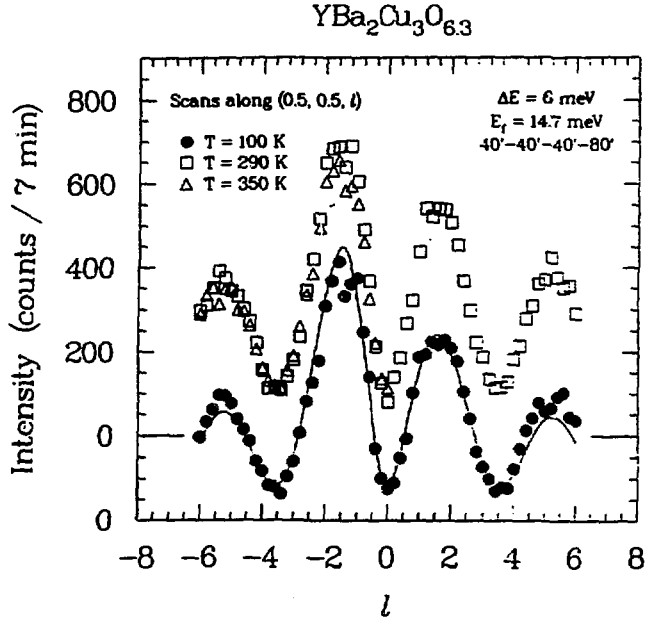

Fig. 12. Constant ΔE scan of type B (see Fig. 9) along the 2D rod with $\Delta E = 6$ meV for $YBa_2Cu_3O_{6.3}$. The modulation is due to the inelastic structure. The enhancement near $l = -1.5$ is due to a "focussing" effect of the spectrometer resolution function. The solid line is a fit which is discussed in the text. From Ref. [40].

(< 75 K) in a powder sample with $x = 0.59$ and $T_c = 47$ K. Fairly strong spin-wave-like scattering was recently observed in a large orthorhombic crystal with $x \sim 0.45$ and $T_c \approx 15$ K [53]; however, initial measurements on several other crystals with larger oxygen concentrations were negative [40]. Brückel *et al.* [54] found negligible magnetic scattering for $|\hbar\omega| < 25$ meV in an $x = 1$ powder sample, and they concluded that most of the Cu atoms are nonmagnetic. However, that conclusion is based on the assumption that most of the magnetic scattering should occur at low energies, whereas spin-wave theory indicates that for the antiferromagnetic tetragonal material most of the spectral weight occurs at $\hbar\omega > J_{\|}$. A short magnetic correlation length or a shift in spectral weight to higher energies could explain the negative observations at low energies. Cu NMR and NQR studies appear to give positive evidence for the presence of interacting Cu^{2+} spins in $YBa_2Cu_3O_7$ [55].

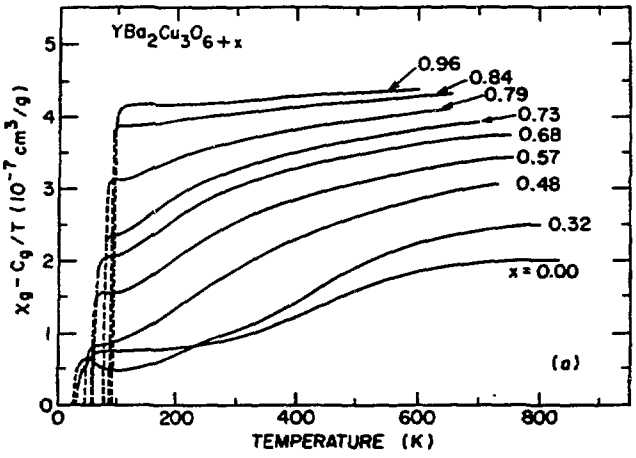

Fig. 13. Magnetic susceptibility, corrected for a Curie-like contribution, plotted vs. temperature for a range of oxygen concentrations in $YBa_2Cu_3O_{6+x}$. From Ref. [30].

5. Summary

The magnetic and electronic correlations in $YBa_2Cu_3O_{6+x}$ are controlled by the oxygen-filling and ordering of the Cu(1)-O_x layers. Oxygen atoms tend to cluster in CuO chains in order to minimize the number 3-fold coordinated coppers. In the orthorhombic phase, ordering of the oxygens in chains creates O $2p$ holes, a large fraction of which are transferred to the CuO_2 planes. Each BaO layer acts as a dielectric which distorts to help screen the charge transfer. The reduction in the number of holes on removal of oxygen is partially compensated by the conversion of $Cu(1)^{2+}$ to $Cu(1)^{1+}$. T_c tends to scale with the density of mobile O $2p$ holes. In the tetragonal phase the chain segments become short and lack orientational order; very few holes are transferred to the planes.

Antiferromagnetism occurs throughout the insulating tetragonal phase. CuO_2 bilayers are coupled antiferromagnetically, and they remain correlated in the absence of long-range order. $Cu(1)^{2+}$ atoms in Cu(1)-O chain segments tend to couple ferromagnetically to the CuO_2 layers at low temperature. Holes in the CuO_2 planes reduce the magnetic correlation length and kill long-range order. Nevertheless, there is evidence that Cu^{2+} moments survive and interact in the metallic state. More work is required to understand the interactions between O $2p$ and Cu $3d$ holes in the metallic phase.

Acknowledgements

I am grateful for interactions and discussions with many colleagues and collaborators, especially including R. J. Birgeneau, V. J. Emery, S. M. Heald, D. C. Johnston, B. Keimer, A. R. Moodenbaugh, A. H. Moudden, M. Sato, G. Shirane, S. K. Sinha, and Y. J. Uemura. This work was supported in part by the U.S.-Japan Cooperative Neutron Scattering Program. Research at Brookhaven in supported by the Division of Materials Sciences, U.S. Department of Energy under contract No. DE-AC02-76CH00016.

References

1. J. G. Bednorz and K. A. Müller, *Z. Phys. B* **64**, 189 (1986).
2. M. K. Wu, J. R. Ashburn, C. J. Torng, P. H. Hor, R. L. Meng, L. Gao, Z. J. Huang, Y. Q. Wang, and C. W. Chu, *Phys. Rev. Lett.* **58**, 908 (1987).
3. M. A. Beno, L. Soderholm, D. W. Capone II, D. G. Hinks, J. D. Jorgensen, J. D. Grace, I. K. Schuller, C. U. Segre, and K. Zhang, *Appl. Phys. Lett.* **51**, 57 (1987); D. E. Cox, A. R. Moodenbaugh, J. J. Hurst, and R. H. Jones, *J. Phys. Chem. Solids* **49**, 47 (1988).
4. D. C. Johnston, A. J. Jacobson, J. M. Newsam, J. T. Lewandowski, D. P. Goshorn, D. Xie, and W. B. Yelon, in *Chemistry of High-Temperature Superconductors*, edited by D. L. Nelson, M. S. Whittingham, and T. F. George, ACS Symposium Series No. 351 (American Chemical Society, Washington, DC, 1987); A. Renault, G. J. McIntyre, G. Collin, J. P. Pouget, and R. Comès, *J. Phys. (Paris)* **48**, 1407 (1987).
5. N. Nishida *et al.*, *Jpn. J. Appl. Phys.* **26**, L1856 (1987); *J. Phys. Soc. Jpn.* **57**, 722 (1988).
6. J. M. Tranquada, D. E. Cox, W. Kunnmann, H. Moudden, G. Shirane, M. Suenaga, P. Zolliker, D. Vaknin, S. K. Sinha, M. S. Alvarez, A. J. Jacobson, and D. C. Johnston, *Phys. Rev. Lett.* **60**, 1567 (1988); J. Rossat-Mignod, P. Burlet, M. J. G. M. Jurgens, J. Y. Henry, and C. Henry, *Physica C* **152**, 19 (1988); W.-H. Li, J. W. Lynn, H. A. Mook, B. C. Sales, and Z. Fisk, *Phys. Rev. B* **37**, 9844 (1988); D. Petitgrand and G. Collin, *Physica C* **153**, 192 (1988).
7. J. L. Hodeau, C. Chaillout, J. J. Capponi, and M. Marezio, *Solid State Commun.* **64**, 1349 (1987).

8. G. Van Tendeloo, H. W. Zandbergen, and S. Amelinckx, *Solid State Commun.* **63**, 603 (1987); T. Takabatake, M. Ishikawa, Y. Nakazawa, and K. Koga, *Physica C* **152**, 424 (1988); D. J. Werder, C. H. Chen, R. J. Cava, and B. Batlogg, *Phys. Rev. B* **37**, 2317 (1988); **38**, 5130 (1988).
9. R. M. Fleming, L. F. Schneemeyer, P. K. Gallagher, B. Batlogg, L. W. Rupp, and J. V. Waszczak, *Phys. Rev. B* **37**, 7920 (1988).
10. L. T. Wille, A. Berera, and D. de Fontaine, *Phys. Rev. Lett.* **60**, 1065 (1988); A. Berera and D. de Fontaine, *Phys. Rev. B* **39**, 6726 (1989); R. Kikuchi and J.-S. Choi (to be published).
11. R. J. Cava, B. Batlogg, C. H. Chen, E. A. Rietman, S. M. Zahurak, and D. Werder, *Phys. Rev. B* **36**, 5719 (1987).
12. Y. Nakazawa and M. Ishikawa, *Physica C* **158**, 381 (1989).
13. R. J. Cava, B. Batlogg, K. M. Rabe, E. A. Rietman, P. K. Gallagher, and L. W. Rupp Jr, *Physica C* **156**, 523 (1988); W. K. Kwok, G. W. Crabtree, A. Umezawa, B. W. Veal, J. D. Jorgensen, S. K. Malik, L. J. Nowicki, A. P. Paulikas, and L. Nunez, *Phys. Rev. B* **37**, 106 (1988); P. F. Miceli, J. M. Tarascon, L. H. Greene, P. Barboux, F. J. Rotella, and J. D. Jorgensen, *Phys. Rev. B* **37**, 5932 (1988).
14. For example, see the review by K. C. Hass, *Solid State Phys.* **42**, (1989).
15. J. A. Yarmoff, D. R. Clarke, W. Drube, U. O. Karlsson, A. Taleb-Ibrahimi, and F. J. Himpsel, *Phys. Rev. B* **36**, 3967 (1987); P. Kuiper, G. Kruizinga, J. Ghijsen, M. Grioni, P. J. W. Weijs, F. M. F. de Groot, G. A. Sawatzky, H. Verweij, L. F. Feiner, and H. Petersen, *Phys. Rev. B* **38**, 6483 (1988).
16. N. Nücker, J. Fink, J. C. Fuggle, P. J. Durham, and W. M. Temmerman, *Phys. Rev. B* **37**, 5158 (1988).
17. N. Nücker, H. Romberg, X. X. Xi, J. Fink, B. Gegenheimer, and Z. X. Zhao, *Phys. Rev. B* **39**, 6619 (1989).
18. M. Takigawa, P. C. Hammel, R. H. Heffner, and Z. Fisk, *Phys. Rev. B* **39**, 7371 (1989).
19. M. Horvatić, Y. Berthier, P. Butaud, Y. Kitaoka, P. Ségransan, C. Berthier, H. Katayama-Yoshida, Y. Okabe, and T. Takahashi (to be published).
20. H. Alloul, P. Mendels, G. Collin, and P. Monod, *Phys. Rev. Lett.* **61**, 746 (1988).
21. L.-S. Kau, D. J. Spira-Solomon, J. E. Penner-Hahn, K. O. Hodgson, and E. I. Solomon, *J. Am. Chem. Soc.* **109**, 6433 (1987).

22. S. M. Heald, J. M. Tranquada, A. R. Moodenbaugh, and Y. Xu, *Phys. Rev. B* **38**, 761 (1988).
23. J. M. Tranquada, S. M. Heald, A. R. Moodenbaugh, and Y. Xu, *Phys. Rev. B* **38**, 8893 (1988).
24. T. A. Smith, J. E. Penner-Hahn, K. O. Hodgson, M. A. Berding, and S. Doniach, in *EXAFS and Near Edge Structure III*, edited by K. O. Hodgson, B. Hedman, and J. E. Penner-Hahn (Springer-Verlag, Berlin, 1984), p. 58.
25. M. K. Kelly, P. Barboux, J.-M. Tarascon, D. E. Aspnes, W. A. Bonner, and P. A. Morris, *Phys. Rev. B* **38**, 870 (1988).
26. W. W. Warren, Jr., R. E. Walstedt, G. F. Brennert, R. J. Cava, B. Batlogg, and L. W. Rupp, *Phys. Rev. B* **39**, 831 (1989).
27. M. Horvatić, P. Ségransan, C. Berthier, Y. Berthier, P. Butaud, J. Y. Henry, M. Couach, and J. P. Chaminade, *Phys. Rev. B* **39**, 7332 (1989).
28. Y. J. Uemura *et al.*, *Phys. Rev. Lett.* **62**, 2317 (1989).
29. Y. Kubo and H. Igarashi, *Phys. Rev. B* **39**, 725 (1989).
30. J. M. Tranquada, A. H. Moudden, A. I. Goldman, P. Zolliker, D. E. Cox, G. Shirane, S. K. Sinha, D. Vaknin, D. C. Johnston, M. S. Alvarez, A. J. Jacobson, J. T. Lewandowski, and J. M. Newsam, *Phys. Rev. B* **38**, 2477 (1988).
31. J. Rossat-Mignod, P. Burlet, M. J. Jurgens, C. Vettier, L. P. Regnault, J. Y. Henry, C. Ayache, L. Forro, H. Noel, M. Potel, P. Gougeon, and J. C. Levet, *J. Phys. Colloq.* **49**, C8-2119 (1988).
32. P. W. Anderson, *Phys. Rev.* **86**, 694 (1952); M. E. Lines, *J. Phys. Chem. Solids* **31**, 101 (1970).
33. J. H. Brewer *et al.*, *Phys. Rev. Lett.* **60**, 1073 (1988).
34. M. Matsumura, H. Yamagata, Y. Yamada, K. Ishida, Y. Kitaoka, K. Asayama, H. Takagi, H. Iwabuchi, and S. Uchida, *J. Phys. Soc. Jpn.* **57**, 3297 (1988); P. Mendels and H. Alloul, *Physica C* **156**, 355 (1988).
35. R. J. Birgeneau and G. Shirane, in *Physical Properties of High Temperature Superconductors I*, edited by D. M. Ginsberg (World Scientific, Singapore, 1989).
36. Y. Guo, J.-M. Langlois, and W. A. Goddard III, *Science* **239**, 896 (1988).
37. A. H. Moudden, G. Shirane, J. M. Tranquada, R. J. Birgeneau, Y. Endoh, K. Yamada, Y. Hidaka, and T. Murakami, *Phys. Rev. B* **38**, 8720 (1988).

38. Y. Lu and B. Patton (to be published).
39. H. Kadowaki, M. Nishi, Y. Yamada, H. Takeya, H. Takei, S. M. Shapiro, and G. Shirane, *Phys. Rev. B* **137**, 7932 (1988).
40. J. M. Tranquada, G. Shirane, B. Keimer, S. Shamoto, and M. Sato, *Phys. Rev. B* (to be published).
41. W. E. Farneth, R. S. McLean, E. M. McCarron, III, F. Zuo, Y. Lu, B. R. Patton, and A. J. Epstein, *Phys. Rev. B* **39**, 6594 (1989).
42. M. Matsumura, H. Yamagata, Y. Yamada, K. Ishida, Y. Kitaoka, K. Asayama, H. Takagi, H. Iwabuchi, and S. Uchida, *J. Phys. Soc. Jpn.* **58**, 805 (1989).
43. H. Lütgemeier and B. Rupp, *J. Phys. Colloq.* **49**, C8-2147 (1988).
44. P. F. Miceli, J. M. Tarascon, L. H. Greene, P. Barboux, M. Giroud, D. A. Neumann, J. J. Rhyne, L. F. Schneemeyer, and J. V. Waszczak, *Phys. Rev. B* **38**, 9209 (1988); P. F. Miceli, J. M. Tarascon, P. Barboux, L. H. Greene, B. G. Bagley, G. W. Hull, M. Giroud, J. J. Rhyne, and D. A. Neumann, *Phys. Rev. B* **39**, 12375 (1989); P. Zolliker, D. E. Cox, J. M. Tranquada, and G. Shirane, *Phys. Rev. B* **38**, 6575 (1988).
45. J. W. Lynn, W.-H. Li, H. A. Mook, B. C. Sales, and Z. Fisk, *Phys. Rev. Lett.* **60**, 2781 (1988); A. H. Moudden, G. Shirane, J. M. Tranquada, R. J. Birgeneau, Y. Endoh, K. Yamada, Y. Hidaka, and T. Murakami, *Phys. Rev. B* **38**, 8720 (1988).
46. P. W. Anderson, *Science* **235**, 1196 (1987).
47. G. Shirane, Y. Endoh, R. J. Birgeneau, M. A. Kastner, Y. Hidaka, M. Oda, M. Suzuki, and T. Murakami, *Phys. Rev. Lett.* **59**, 1613 (1987); Y. Endoh *et al.*, *Phys. Rev. B* **37**, 7443 (1988).
48. K. B. Lyons, P. A. Fleury, L. F. Schneemeyer, and J. V. Waszczak, *Phys. Rev. Lett.* **60**, 732 (1988).
49. M. Sato, S. Shamoto, J. M. Tranquada, G. Shirane, and B. Keimer, *Phys. Rev. Lett.* **61**, 1317 (1988).
50. D. C. Johnston, S. K. Sinha, A. J. Jacobson, and J. M. Newsam, *Physica C* **153-155**, 572 (1988).
51. See, for example, L. J. de Jongh and A. R. Miedema, *Adv. Phys.* **23**, 1 (1974).
52. F. Mezei, B. Faragó, C. Pappas, Gy. Hutiray, L. Rosta, and L. Mihály, *Physica C* **153-155**, 1669 (1988).
53. J. M. Tranquada, H. Chou, G. Shirane, S. Shamoto, and M. Sato (unpublished).

54. T. Brückel, H. Capellmann, W. Just, O. Schärpf, S. Kemmler-Sack, R. Kiemel, and W. Schaefer, *Europhys. Lett.* **4**, 1189 (1987).
55. See, for example, F. Mila and T. M. Rice, *Physica C* **157**, 516 (1989).